# Aeroelastic code comparison using the IEA 22MW reference turbine



Journal of Physics: Conference Series **2767** (2024) 052042 doi:10.1088/1742-6596/2767/5/052042

# Aeroelastic code comparison using the IEA 22MW reference turbine

**W Collier[1], D Ors[1], T Barlas[2], F Zahle[2], P Bortolotti[3], D Marten[4], C S L Jensen[1], E Branlard[3], D Zalkind[3], K Lønbæk[2]**

[1] DNV Services UK Limited, United Kingdom
[2] Department of Wind and Energy Systems, Technical University of Denmark
[3] National Renewable Energy Laboratory, Golden CO, USA
[4] Technical University of Berlin, Chair of Fluid Dynamics, Mueller-Breslau Strasse 8, 10623 Berlin, Germany

email: william.collier@dnv.com

**Abstract**. Reference wind turbine designs and the associated aeroelastic models are widely used in both research and industry. Reference models representing future concepts are of particular interest. Current state of the art aeroelastic tools are relied upon to design the next generation of large wind turbines. However, modelling assumptions may be invalidated by upcoming very large turbines, and different aeroelastic tools may give inconsistent results. A 22MW turbine model has been defined as part of International Energy Agency (IEA) Wind Task 55 on Reference Wind Turbines and Farms to represent future turbines to be deployed in the 2030s. In this study, an aeroelastic model of this turbine has been created in four tools; Bladed, HAWC2, OpenFAST, and QBlade. Code comparisons are presented for steady state operation, linear stability analysis, and time domain power production simulations in steady and turbulent wind. Generally, the codes show a good agreement, but with some differences present in the linear stability analysis, periodic azimuthal variation, and time domain simulations. The models are a good basis for further study with the IEA 22MW turbine, and further code comparison exercises.

## 1. Introduction and motivation

Reference wind turbine (RWT) designs such as the IEA 15-MW RWT [1] and the Denmark Technical University (DTU) 10-MW RWT [2], and their associated aeroelastic models, are widely used in both research and industry. Research applications include the study of novel concepts or advanced physics models such as in IEA Wind Technology Collaboration Programme (TCP) Task 47 [3], whereas industrial applications include deriving concept loads for preliminary floating sub-structure design.

Reference aeroelastic models representing future concepts are of particular interest. Current state of the art aeroelastic tools are relied upon to design the next generation of large wind turbines. However, modelling assumptions may be invalidated by upcoming very large turbines [4]. For example, high blade flexibility can introduce uncertainty due to comparably larger blade torsional deformations and challenge aerodynamic assumptions in blade element momentum models.

A 22 MW turbine, the IEA 22 MW RWT has been designed as part of IEA Wind TCP Tasks 37 and 55 [5] to represent future turbines to be deployed in the 2030s. The turbine includes detailed design of all major components, and its properties are described in sufficient detail for aeroelastic modelling of the full turbine. In this study, the aeroelastic model has been created in four widely used tools: Bladed [9], HAWC2 [10], OpenFAST [11], and QBlade [12]. Code comparisons of operating conditions and

loads are presented for the IEA 22 MW RWT for steady state operation, linear stability analysis, and time domain operation with steady wind and turbulent wind. This broad range of comparisons aims to:

- Evaluate the level of tool consistency when the same design is modelled in different tools
- Expose differences between the tools that may not be present for current generation turbines, and so identify areas for further detailed study
- Demonstrate that the RWT design is stable in a variety of aeroelastic tools
- Provide a baseline set of comparisons to aid researchers using other aeroelastic tools
- Provide the created models to tool users as a basis for further studies

## 2. Turbine definition and tools

In this section, the turbine model definition is described. The studied aeroelastic codes are introduced.

### 2.1. Turbine definition

The IEA 22 MW RWT is an upwind, three-bladed, direct-drive wind turbine. Its rated power is 22 MW, the rotor diameter is 284 m, and the rated wind speed is 11.5 m/s. The rotor has a cone angle of 4 degrees and a tilt angle of 6 degrees. The blade prebend is 7 m at the tip. The control strategy is variable speed pitch regulated. A tubular tower and monopile are defined, resulting in a hub height of 170 m above sea level. The water depth is assumed as 34 m, with a rigid foundation condition at the seabed. A full description of the turbine is available in a report from IEA Task 55[15]. The model definition is available on GitHub [6] in WindIO [7] format. In this work, v1.0.0 of the turbine is used.

### 2.2. Studied aeroelastic codes

Bladed, HAWC2, OpenFAST and QBlade are low to mid fidelity engineering modelling tools. Designed for numerical efficiency, these tools run relatively quickly to be able to cover a large range of predominantly time domain load cases in a reasonable time.

All of the tools use flexible multibody dynamics formulations, with flexible components modelled using beam elements. There are various formulations to model geometrically non-linear deformations in the blades. Blade cross section parameters are provided to the tools either at the locations of structural centres, or as fully populated 6x6 cross section matrices. In this study, aerodynamics are modelled using blade element momentum theory. The turbine controller is included via a Dynamic Link Library (DLL). Details about the sub-models selected in each tool for this study are provided in Table 1.

Table 1. Summary of selected modelling options of the studied aeroelastic tools in this study.

| | **Bladed** | **HAWC2** | **OpenFAST** | **QBlade** |
|---|---|---|---|---|
| **Aerodynamics formulation** | Blade element momentum theory. Beddoes Leishman style dynamic stall. | Blade element momentum polar grid. Beddoes Leishman style dynamic stall. | Blade element momentum. Beddoes Leishman style dynamic stall. | Blade element momentum polar grid. Øye style dynamic stall. |
| **Non-linear blade deformation model** | Multiple bodies with linear Timoshenko beam elements in floating frame of reference formulation. | Multiple bodies with linear Timoshenko beam elements in floating frame of reference formulation. | BeamDyn: Geometrically exact beam theory for arbitrarily large displacement. | Multiple linear Timoshenko beam elements in co-rotational formulation. |
| **Blade cross section parameterisation** | Location and orientation of elastic, shear, mass centres | 6x6 stiffness matrix at elastic centre. Mass centre location and orientation. | 6x6 mass and stiffness matrix at reference axis. | 6x6 mass and stiffness matrix at reference axis. |
| **Control system** | ROSCO controller 2.8.0 [14] | DTU Wind Energy Controller [13] | ROSCO controller 2.9.0 [14] | DTU Wind Energy Controller [13] |

| | | | | |
|---|---|---|---|---|
| **Tower and monopile structural formulation** | Single linear finite element body for tower and monopile. Timoschenko beams with modal reduction. | Separate linear finite element bodies for tower and monopile. Timoschenko beams, no modal reduction. | Tower: ElastoDyn: Linear body with 4 bending modes. Monopile: SubDyn: Linear finite element & Guyan reduction. | Analogue to blade model: Multiple linear Timoshenko beams for tower and monopile bodies. |
| **Software version** | 4.14.0.3 | 13.0.7 (HAWC2) 2.16 (HAWCStab2) | 3.5.3 | 2.0.7 |

## 3. Test cases

Test cases are defined covering comparisons of masses, frequencies, steady state parameters, linearised stability analysis, azimuthal variation, and time domain with turbulent wind. Output coordinate systems are defined for blade section loads and deformations and applied aerodynamic loads.

### 3.1. Mass, inertia and structural frequencies

Mass totals are calculated for blade, rotor nacelle assembly, tower, monopile, and whole support structure. Blade mass moments are calculated around the blade root y axis, as shown in Figure 1. The results are presented in Table 2. Structural frequencies in a vacuum are calculated for an isolated blade, and for the whole turbine with flexible support structure but rigid rotor nacelle assembly (RNA), rotor locked and pitch angle = 0. The results are presented in Table 3 and Table 4.

### 3.2. Steady state operation

Steady state operating conditions are found for the turbine operating between 3 and 25 m/s. The steady rotor speed and pitch angle at each windspeed are prescribed in HAWC2, obtained in time domain simulations in OpenFAST and QBlade, and calculated from steady state control parameters in Bladed. The inflow is uniform, and the tilt angle is set to zero. Gravity it not included. The blade is considered flexible, but the support structure is modelled as rigid. The converged steady state values for rotor power, torque, thrust, blade loads, and blade deformations are presented in Figure 2 and Figure 3.

### 3.3. Periodic variation with azimuth angle

Time domain simulations are performed under uniform inflow conditions at 10m/s wind speed. The blade is considered flexible, but the support structure is modelled as rigid. Some sources of periodic variation are introduced and the variation of output parameters with azimuth angle is studied. The sources of periodic loading are gravity, rotor tilt and tower shadow. Dynamic stall and wake models are activated. Wind shear, upflow and yaw misalignment are excluded. The presented outputs are blade root loads, blade tip deformation, and blade rotational deformation and angle of attack at 80% blade length. The results are presented in Figure 4.

### 3.4. Linear stability analysis

Steady state operating conditions are found with environmental conditions and model setup identical to those described in section 3.2. A numerical linearisation is performed, giving an output of coupled mode frequencies and damping ratios. The results include dynamic aerodynamic effects due to stall and wake. No QBlade results are presented for this case. The results are presented in Figure 5.

### 3.5. Time domain operation with turbulent wind

Power production simulations of duration 10 minutes are carried out at wind speeds of 3-25m/s. Turbulent wind according to class B conditions [8] is used, with normal turbulence model (NTM). HAWC2 uses Mann turbulence whereas Bladed, OpenFAST, and QBlade use Kaimal turbulence. 18 turbulent realisations are used at each wind speed, 6 each at yaw misalignments of -8, 0 and +8 degrees. Wind shear power law exponent is 0.14. No upflow is included. Tower shadow effects are included. The turbine blades and tower are modelled as flexible. Tilt angle is included. All dynamic models such as

aerodynamic stall and dynamic wake are enabled. Turbine controller DLLs are used to control the turbine. Peak values, standard deviation, mean and damage equivalent load are calculated for each realisation, then averaged across the 18 realisations. The results are shown in Figure 6 and Figure 7.

### 3.6. Coordinate systems

The following coordinate systems are used for all relevant outputs presented in this paper.

*3.6.1. Blade deformation and loads coordinates.* The output system for blade deformation and root loads follows the system shown in Figure 1. Blade rotational deformations are given as three components of a single rotation around an axis, expressed as a vector of rotational deformations (x,y,z). Along the blade, the origin of the load output system is at the blade reference axis positions as defined in the WindIO blade definition. The orientation of the load output system is always aligned with the blade root system, as it rotates with pitch angle.

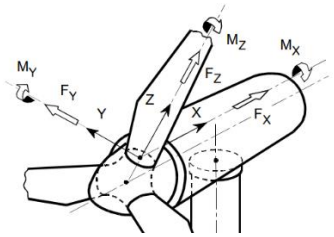


Figure 1. Blade root coordinate system. The Z direction follows the pitch axis. At zero pitch, the X direction points downwind. The system rotates with pitch angle.

*3.6.2. Blade aerodynamic forces.* The tangential and axial aerodynamic forces along the blade are reported in a plane perpendicular to the rotor axis.

## 4. Results

Table 2. Mass and inertia comparisons for the turbine

| | **Bladed** | **HAWC2** | **OpenFAST** | **QBlade** | **Max error %** |
|---|---|---|---|---|---|
| **Blade mass (Kg)** | 8.243E+04 | 8.156E+04 | 8.262E+04 | 8.242E+04 | 1.3 |
| **Blade 1st moment mass (Kgm)** | 3.034E+06 | 3.033E+06 | 3.068E+06 | 3.045E+06 | 1.1 |
| **Blade 2nd moment mass (Kgm$^2$)** | 2.048E+08 | 2.052E+08 | 2.049E+08 | 2.059E+08 | 0.5 |
| **RNA mass (Kg)** | 1.217E+06 | 1.215E+06 | 1.218E+06 | 1.218E+06 | 0.3 |
| **Tower mass (Kg)** | 1.574E+06 | - | 1.577E+06 | 1.574E+06 | 0.2 |
| **Monopile mass (Kg)** | 1.090E+06 | - | 1.062E+06 | 1.090E+06 | 2.7 |
| **Tower + monopile mass (Kg)** | 2.665E+06 | 2.663E+06 | 2.639E+06 | 2.665E+06 | 1.0 |

Table 3. Isolated blade mode frequencies in Hz, and damping ratio % in brackets

| Mode | **Bladed** | **HAWCStab2** | **OpenFAST** | **QBlade** | **Max error %** |
|---|---|---|---|---|---|
| **1st flapwise** | 0.385 (0.491) | 0.384 (0.502) | 0.386 (0.491) | 0.384 (0.510) | 0.6 (3.8) |
| **1st edgewise** | 0.518 (0.507) | 0.520 (0.506) | 0.520 (0.507) | 0.515 (0.510) | 1.0 (0.8) |
| **2nd flapwise** | 1.058 (1.336) | 1.060 (1.360) | 1.066 (1.336) | 1.058 (1.365) | 0.8 (2.2) |
| **2nd edgewise** | 1.486 (1.364) | 1.440 (1.290) | 1.495 (1.364) | 1.483 (1.404) | 3.7 (8.4) |
| **3rd flapwise** | 2.210 (2.749) | 2.221 (2.860) | 2.229 (2.749) | 2.210 (2.828) | 0.9 (4.0) |
| **3rd edgewise** | 3.200 (2.857) | 3.121 (2.820) | 3.219 (2.857) | 3.195 (3.038) | 3.1 (7.5) |
| **4th flapwise** | 3.667 (3.555) | 3.744 (4.730) | 3.726 (3.555) | 3.673 (3.834) | 2.1 (30.0) |
| **1st torsional** | 3.972 (1.896) | 3.961 (2.000) | 3.981 (1.896) | 3.952 (1.903) | 0.7 (5.4) |

Table 4. Support structure (with rigid RNA) mode frequencies in Hz, and damping ratio % in brackets

| | Bladed | HAWCStab2 | OpenFAST | QBlade | Max error % |
|---|---|---|---|---|---|
| **1st side-side** | 0.160 (0.091) | 0.161 (0.092) | 0.161 (0.116) | 0.161 (0.091) | 0.6 (0.6) |
| **1st fore-aft** | 0.162 (0.091) | 0.163 (0.091) | 0.162 (0.116) | 0.163 (0.091) | 0.4 (0.1) |
| **1st torsional** | 0.690 (0.520) | 0.663 (1.543) | - (-) | 0.660 (0.520) | 4.4 (118) |
| **2nd side-side** | 0.739 (0.519) | 0.725 (0.514) | 0.741 (0.224) | 0.736 (0.519) | 1.8 (0.9) |
| **2nd fore-aft** | 0.806 (0.545) | 0.820 (0.544) | 0.822 (0.286) | 0.811 (0.545) | 1.7 (0.1) |
| **3rd side-side** | 1.649 (1.112) | 1.624 (1.093) | - (-) | 1.636 (1.112) | 1.5 (1.7) |
| **3rd fore-aft** | 1.740 (1.218) | 1.757 (1.226) | - (-) | 1.718 (1.218) | 2.3 (0.6) |
| **4th side-side** | 3.640 (2.501) | 3.611 (2.460) | - (-) | 3.589 (2.501) | 1.4 (1.6) |
| **4th fore-aft** | 3.668 (2.501) | 3.660 (2.504) | - (-) | 3.620 (2.501) | 1.3 (0.1) |

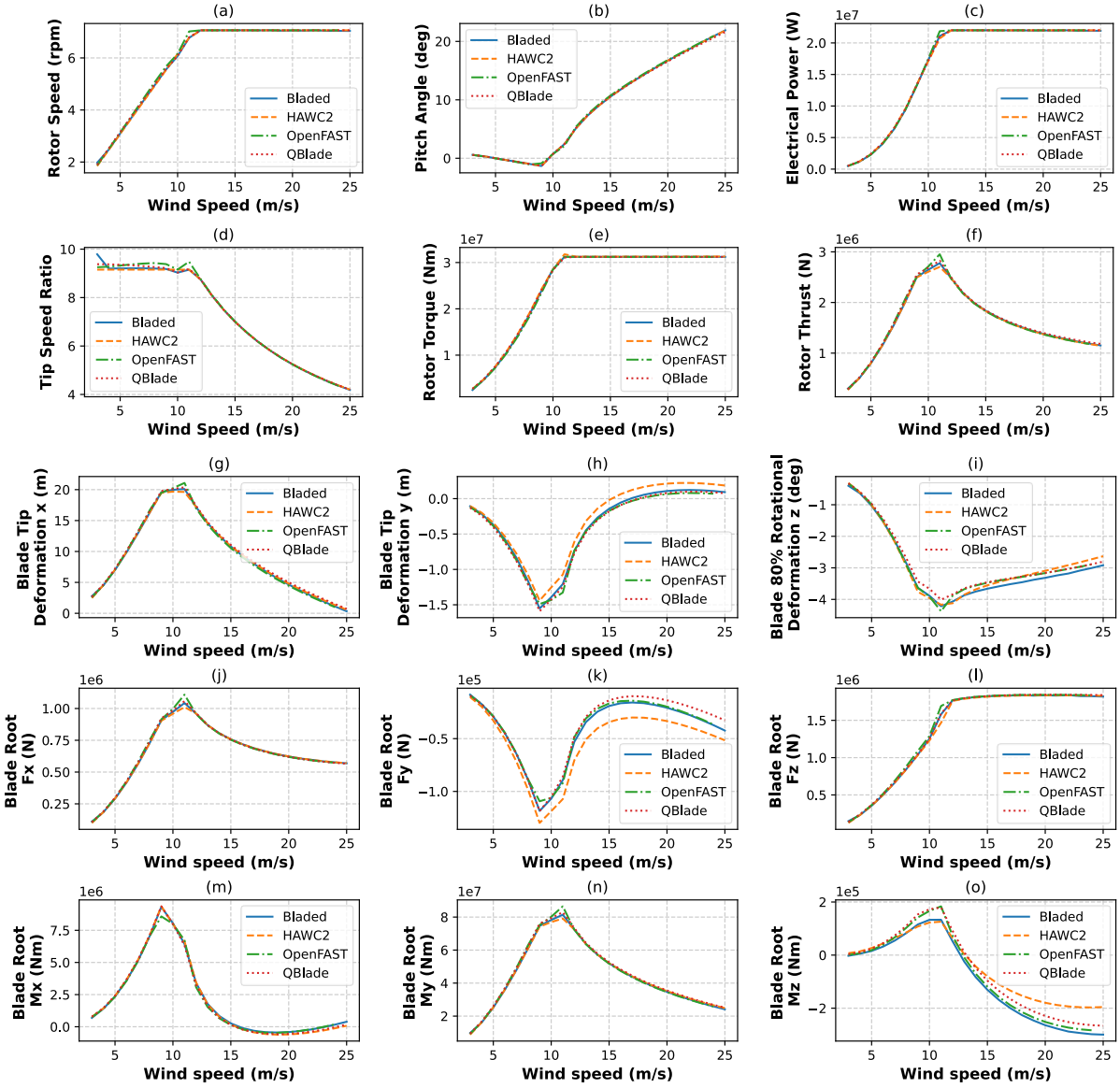


Figure 2. Steady state operation outputs vs wind speed.

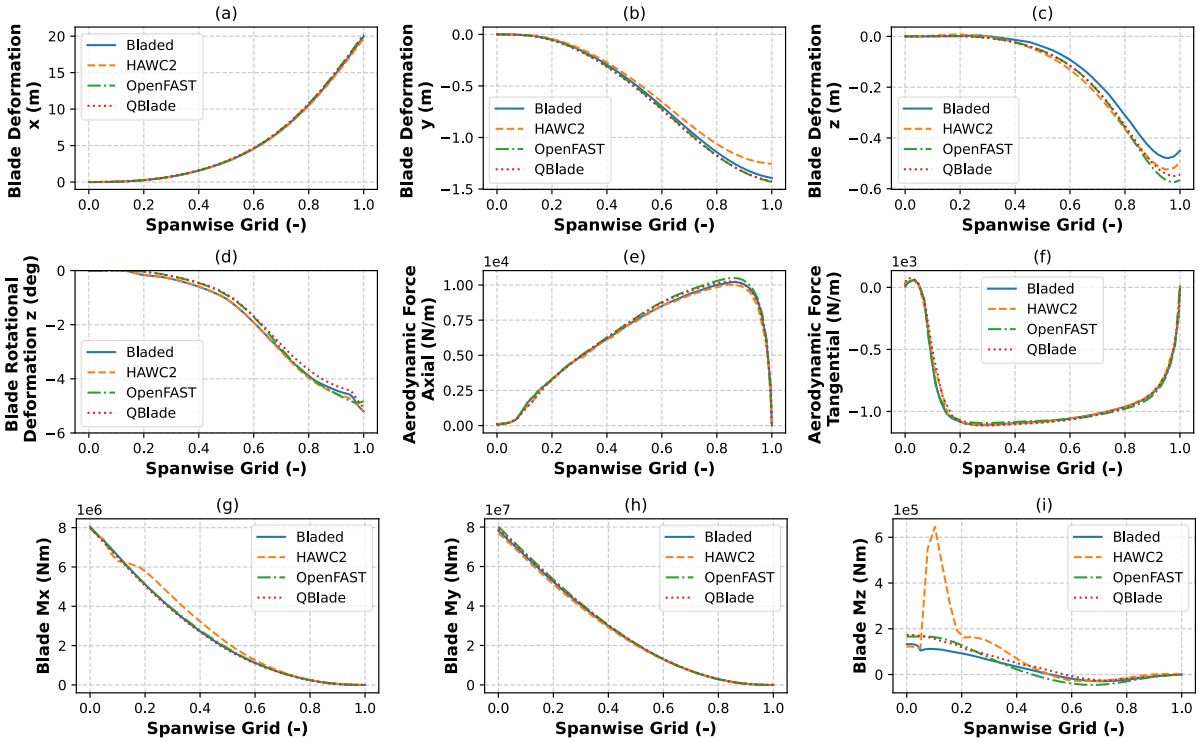


Figure 3. Steady state spanwise blade loads, deformations, and aero loads at 10 m/s wind speed

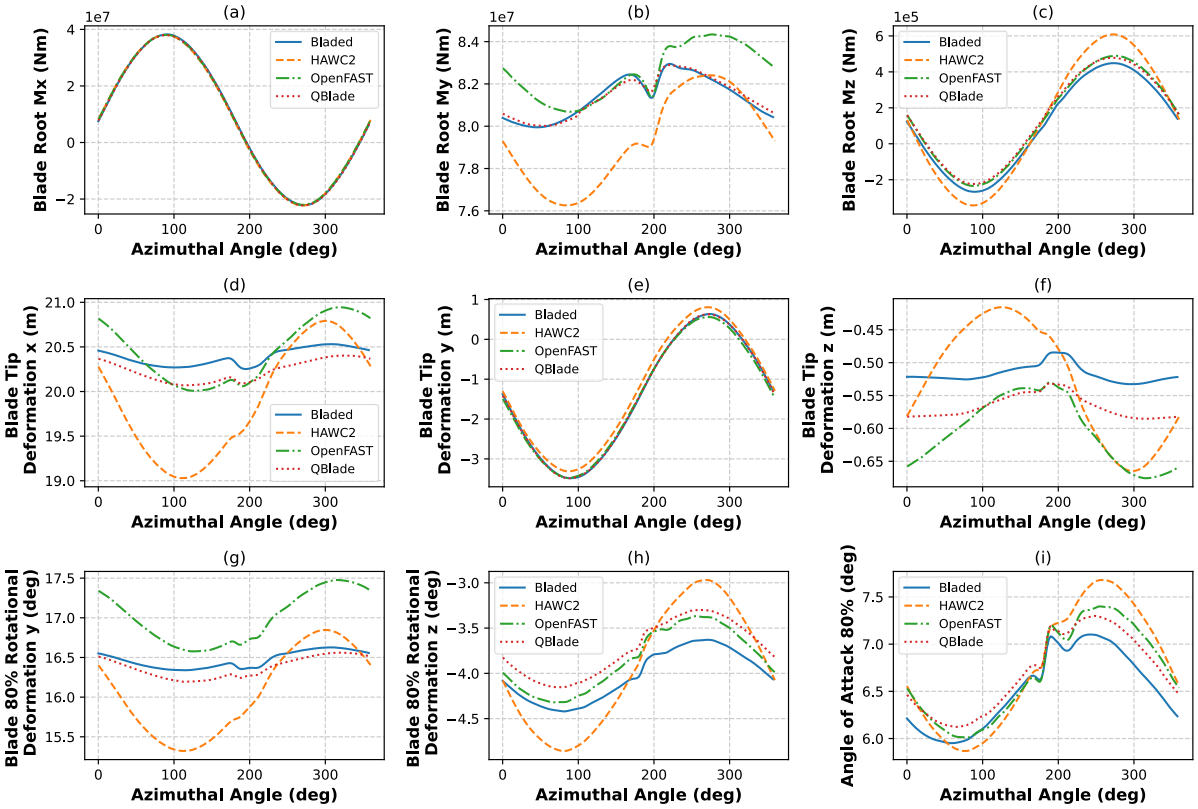


Figure 4. Periodic variation of blade loads, deformations, and angle of attack at 10 m/s wind speed

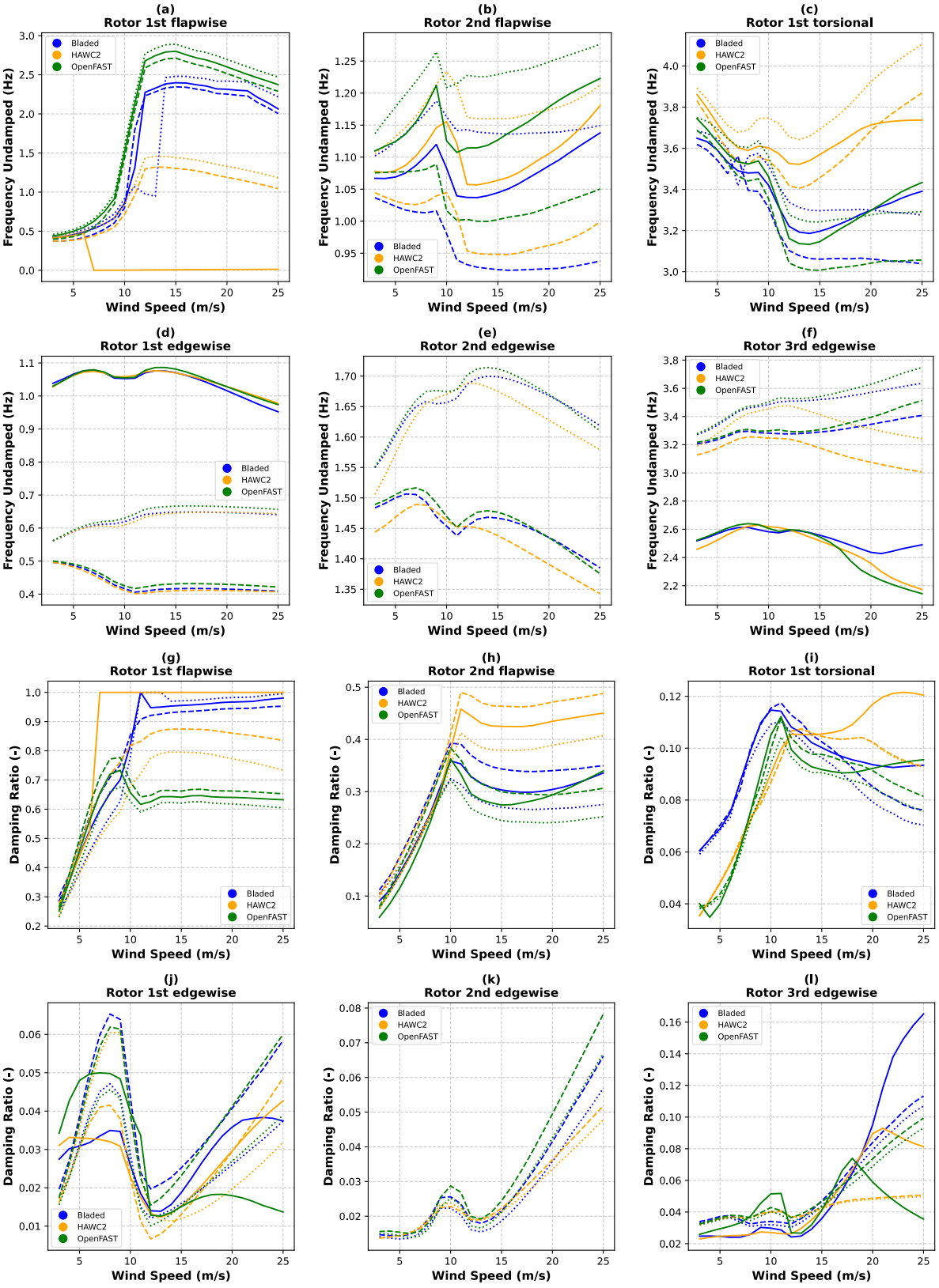


Figure 5. Linear stability analysis with rigid tower. Solid lines represent collective modes. Dotted and dashed lines represent forward and backward collective whirling modes, respectively.

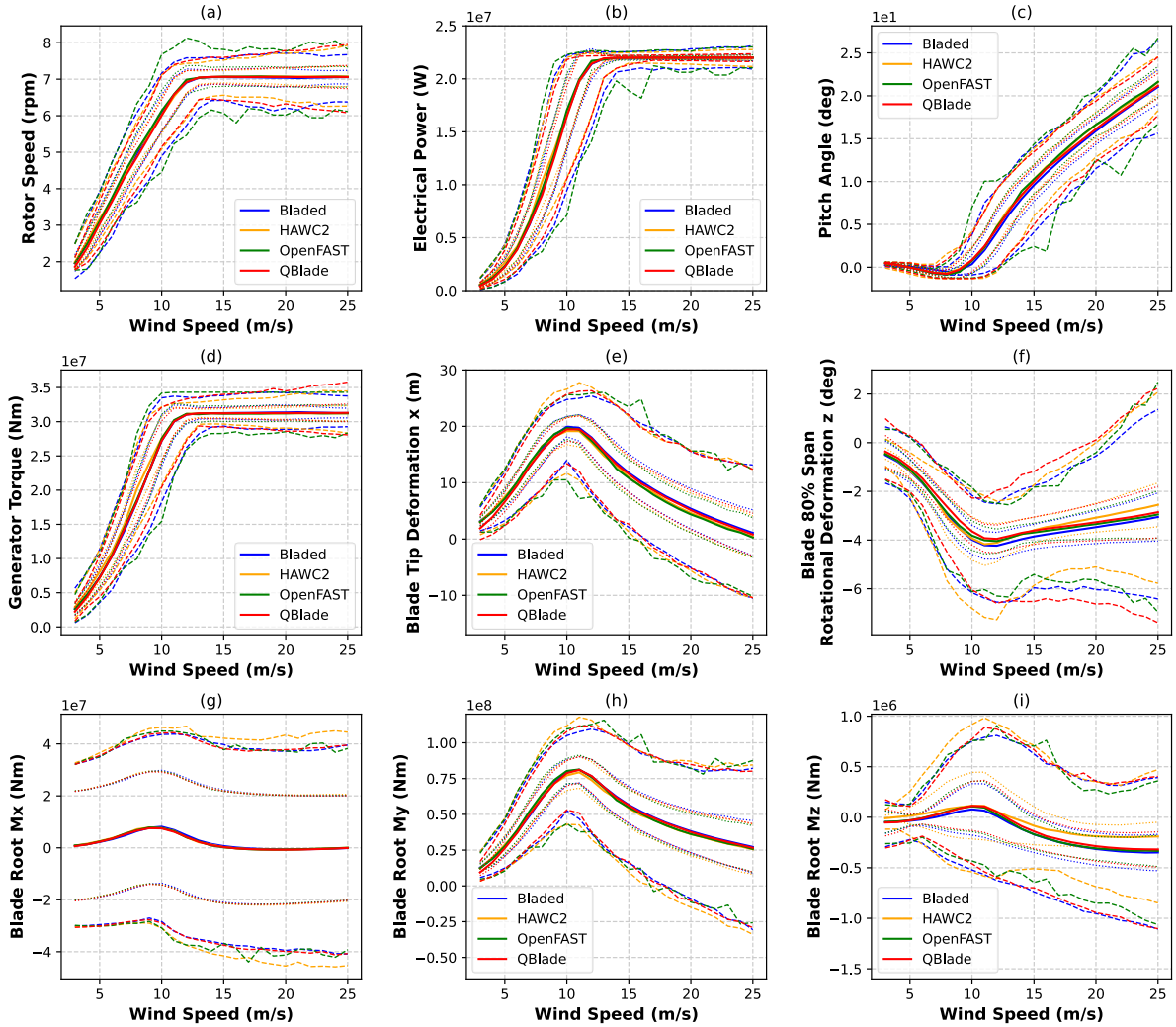


Figure 6. Statistics from time domain operation in turbulent wind. Means are shown with solid lines. Minima and maxima are shown as dashed lines. Standard deviations are shown by the dotted lines.

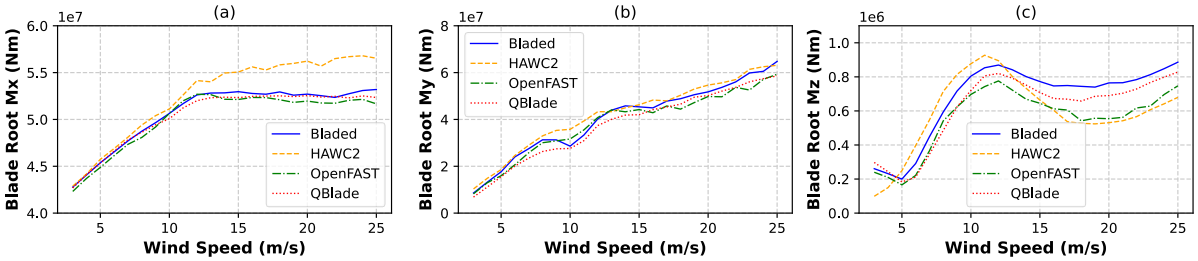


Figure 7. Damage equivalent loads at the blade root from time domain operation in turbulent wind. Evaluated at frequency f = 1Hz and slope m=10.

## 5. Discussion

Mass and inertia outputs are compared in Table 2. The frequency error is calculated as the $(max - min)/mean$ on each row. The agreement is good across the codes. Blade mass differs by up to 1.3%, with HAWC2 differing the most from other codes. This is thought to be due to coarse discretisation of the mass distribution near the blade root. The blade 1st and 2nd moment of mass agree

within 1.1%. RNA mass and "tower + monopile" masses are within 1%. OpenFAST drives the 2.7% difference in monopile mass. Bladed and QBlade agree within 0.01% for all masses.

Structural frequencies and damping for the isolated blade are shown in Table 3. The first three blade mode and torsional frequencies agree within 1% between the codes. HAWC2 shows differences up to 3.7% for 2nd and 3rd edgewise modes. Blade damping is in fairly good agreement with up to 8.3% difference across all modes, except 4th flapwise that shows a 29% maximum difference.

Structural frequencies and damping for the support structure with rigid RNA are shown in Table 4. The 1st bending modes match within 0.6% and higher bending modes within 2.3%. OpenFAST only includes the 1st and 2nd bending modes in the ElastoDyn tower model, so cannot resolve the correct frequencies for 3rd and 4th bending modes or torsion. Bladed has a 4.4% frequency difference from HAWC2 and QBlade for the 1st torsion mode.

Steady state operation is shown in Figure 2. The overall agreement is good. Differences in tip speed ratio (TSR) are observed in plot (d), with OpenFAST showing higher TSR below rated, and Bladed showing a difference at 3m/s wind speed. At 11m/s wind speed, OpenFAST has a higher rotor speed than the other codes in plot (a), leading to higher power, thrust, blade x deformation and blade root Fx and My loads. In plot (i) QBlade shows approximately 0.2 degrees lower torsional deformation than the other codes around rated power. In plot (o), blade root Mz loads show differences. Mz is hard to predict as the scale is 1-2 orders of magnitude smaller than the orthogonal components.

Steady state blade spanwise deformations and loads are shown in Figure 3. The overall agreement is very good. Small differences are seen for the blade deformations in plots (b), (c) and (d). Blade loads Mx and Mz in plots (g) and (i) show differences for HAWC2. This is due to differences in output coordinate system and difficulties with processing the data into the desired output system.

Periodic variation with azimuth at 10m/s wind is shown in Figure 4. The agreement is good for gravity driven outputs such as blade root Mx and blade tip y deformation in plots (a) and (e). For blade root My in plot (b), Bladed and QBlade agree well. OpenFAST has a similar mean value but different azimuthal variation and HAWC2 shows larger differences in both. For blade x deformation and rotational y deformation in plot (d) and (g), Bladed and QBlade agree well with slight mean offset, while HAWC2 and OpenFAST show larger azimuthal variation. For blade rotational z deformation and angle of attack in plots (h) and (i) a consistent mean value is seen. Bladed, OpenFAST and QBlade show similar azimuthal variation. Overall the main outlier in this case is HAWC2. A potential cause is the transformation from the HAWC2 coordinate system into the pitching blade root system (Figure 1).

Linear stability analysis results in operation are shown in Figure 5. The edgewise and torsion mode frequencies match well for Bladed and OpenFAST in plots (c) (d) (e) and (f) , except for the 3rd edgewise collective above 15m/s wind speed. HAWC2 shows differences for the torsion and 2nd and 3rd edgewise modes frequencies, especially at higher wind speeds. Damping trends for edgewise modes are similar between the codes in plots (j) (k) and (l), with the greatest discrepancies seen for the collective modes. The overall trends in 1st torsional mode damping show some agreement in plot (i), but Bladed shows higher damping below rated speed, and HAWC2 higher damping above rated speed. The 1st flapwise mode frequencies show large differences in plot (a). This is thought to be due to difference in how the codes calculate damping for very highly damped modes. The trends for 2nd flapwise mode frequencies in plot (b) agree well with some offset in frequency up to 0.1Hz. Flapwise mode damping ratios show similar trends but different damping ratios in plot (g) and (h).

Time domain operation statistics in turbulent wind are shown in Figure 6. The overall agreement is good, particularly for mean and standard deviation, with some slightly larger differences observed for peak values. Agreement for rotor speed, electrical power, pitch angle and generator torque is good in plots (a) to (d), apart from some OpenFAST peak values. Between rated and cut-out wind speeds, QBlade and HAWC2 show increasing peak generator torque and rotor speed, but this is not seen in Bladed and OpenFAST, which instead show larger peak pitch angles near cut-out wind speed. This may be caused by different control strategies; HAWC2 and QBlade used the DTU WEC whereas Bladed and OpenFAST use the ROSCO controller. Blade tip x deformation agrees well in plot (e). Torsional

deformation about z matches quite well in plot (f), with some disagreement up to 2 degrees in peak values. For blade root Mx in plot (g), HAWC2 shows more extreme peaks, which may indicate greater blade edgewise excitation in HAWC2. A good agreement is seen for blade root My in plot (h). For blade root Mz, HAWC2 shows different mean and peak loads from the other codes.

Damage equivalent loads (DELs) at the blade root are shown in Figure 7. Blade My DELs agree well in plot (b), with the greatest differences around rated speed. Blade Mx DELs are higher in HAWC2 above rated in plot (a), which would be significant for blade root fatigue life. Blade Mz DELs show similar trends but moderate differences in (c), which could be impactful for pitch actuator design.

## 6. Conclusion

Outputs from aeroelastic models of the IEA 22MW RWT in Bladed, HAWC2, OpenFAST and QBlade have been compared. The agreement is very good for steady state and structural frequencies, showing that the basic input parameters are well aligned between the models in each code. The more complex tests highlight greater differences. Periodic azimuthal variation generally agreed well, with HAWC2 being the main outlier possibly due to a required coordinate system transformation. Linear stability analysis showed good agreement in trends for frequency for edgewise and torsional modes, which are important for stability assessment, particularly for Bladed and OpenFAST. Torsional and edgewise damping showed more variation between the codes, particularly for collective modes. Overall there is significant uncertainty in the linear analysis which warrants further study. The time domain statistics and generally agree well, with the largest differences in peak values. Time domain blade DELs agree well, except that HAWC2 shows larger blade root edgewise fatigue damage at high wind speeds.

Steady state analyses have been shown to be a useful first check of model alignment. Agreement for more complex cases is generally good, but individual discrepancies demonstrate that uncertainty in aeroelastic tool outputs for large turbines should be evaluated by using more than one tool. It will be valuable to further investigate the sources of discrepancies to establish whether they are caused by differences in inputs, output conventions or physics models and their specific implementation.

## References

[1] Gaertner, Evan et al 2020. Definition of the IEA 15-Megawatt Offshore Reference Wind. Golden, CO: National Renewable Energy Laboratory. NREL/TP-5000-75698
[2] Bak, C et al (2012). Light Rotor: The 10-MW reference wind turbine. In Proceedings of EWEA 2012 - European Wind Energy Conference & Exhibition European Wind Energy Association
[3] Boersma et al., Progress in the validation of rotor aerodynamic codes using field data, Wind Energy Science, 8, 211–230, 2023 https://wes.copernicus.org/articles/8/211/2023/
[4] Veers, P et al., Grand challenges in the design, manufacture, and operation of future wind turbine systems, Wind Energ. Sci., 8, 1071–1131, https://doi.org/10.5194/wes-8-1071-2023, 2023.
[5] IEA Wind Task 37 https://iea-wind.org/task37/, IEA Wind Task 55 https://iea-wind.org/task-55/
[6] IEA Task 37 2020 IEA GitHub https://github.com/IEAWindTask37/IEA-22-280-RWT
[7] IEA Wind Task 37 2020 WindIO documentation https://windio.readthedocs.io/en/latest/
[8] IEC 61400-1:2019 Wind energy generation systems – Part 1: Design requirements
[9] Bladed https://www.dnv.com/services/wind-turbine-design-software-bladed-3775
[10] T. Larsen and A. Hansen, “How 2 HAWC2, the user’s manual,” Risø National Laboratory, Tech. Rep. 1597(ver. 13.0)(EN), 2023
[11] OpenFAST https://www.nrel.gov/wind/nwtc/openfast.html
[12] D. Marten, 2020, “QBlade: A Modern Tool for the Aeroelastic Simulation of Wind Turbines“, PhD Thesis, TU Berlin, http://dx.doi.org/10.14279/depositonce-10646
[13] Meng F, Lio WH, Barlas T. DTUWEC: an open-source DTU Wind Energy Controller with advanced industrial features. Journal of Physics: Conference Series. 2020;1618:022009.
[14] NREL ROSCO controller https://rosco.readthedocs.io/en/latest/
[15] DTU Wind Energy Report E-0243, ISBN: 978-87-87335-71-3